scientific reports

Check for updates

OPEN

Management practices and elevated atmospheric CO_2 levels helped to sustain a high level of global rice production

Tzu-Shun Lin[1,2] & Atul K. Jain[1]✉

Rice is a staple agricultural resource for over half the global population. Using the data-modeling methods, which account for major biophysical processes and all major environmental and management factors, our study shows that rice production for 2006–2015 has increased by almost 2-fold since the 1960s, despite growing concerns about climate change and other extreme climate event risks. Management practices through the expansion of irrigated and non-irrigated cropping harvested areas and the increased rates of N fertilizer and manure application have helped to maintain higher production rates since the 1960s. The global production of rice for the decade 2006–2015 was 713 million tons per year, with South and Southeast Asia by far the largest rice-producing region, and China (24%), India (22%), and Thailand (9%) being the top three producers. Multiple cropping increases overall production, with the highest rice yield in season one due to a longer growing period and favorable conditions, while yields decline in the subsequent seasons. The results show that global transplanted rice yields are 25% higher than direct-seeded rice yields. Accounting for the effects of management factors, the total production increased by 76%. The expansion of rice-planting areas was the primary management contributing factor (52%), with the expansion of irrigated planted areas contributing 39% and rainfed 13%. Other management practices that helped increase production include N fertilizer and manure (24%). Our results also reveal that environmental factors increased productivity by 24% in the recent decade, with rising atmospheric CO_2 concentration increasing productivity by 30% and N deposition by 1%. In contrast, climate change reduced production by 7%. These findings highlight the critical role of management practices, especially the expansion of irrigated areas and fertilizer use, in driving recent increases in rice production. Accounting for these factors is crucial for accurate projections and effective rice cultivation planning.

Keywords Rice production, Environmental factors, Management factors, Nitrogen fertilizer, Irrigation, ISAM

Rice is one of the leading crops that provides a significant portion of dietary consumption for over half of the world's population[1]. Future rice demand will accelerate with population, technology, and economic growth. However, maintaining the current global rice production is challenging because the yield stagnates. The increase in rice yield has been maintained since 1990[2], and about 35% of the global rice harvested area is currently under stagnation[3]. Furthermore, expected water scarcity and climate change will make rice production more vulnerable to yield losses[4,5]. Understanding how the rice production system has historically been improved or stagnated in response to external environmental and management forces, such as climate change, rising atmospheric CO_2 concentration, crop planting area expansion, irrigation, and N application, would facilitate the identification of critical constraints for future production potential.

Process-based crop models have been developed that account for rice growth processes with comprehensive phenology and their interactions with carbon (C), nitrogen (N), water, and energy cycles, and applied at the site, regional, and global scales to estimate rice yield[6–10]. The global gridded crop model intercomparison (GGCMI) study of the Agricultural Model Intercomparison and Improvement Project (AgMIP)[11,12], which evaluated rice

[1]Department of Climate, Meteorology, and Atmospheric Sciences (CLiMAS), University of Illinois Urbana-Champaign, Urbana, IL, USA. [2]Now at NSF National Center for Atmospheric Research (NCAR), Boulder, CO, USA. ✉email: jain1@illinois.edu

yield from eleven process-based crop growth models, found that the models encounter challenges in evaluating rice yield variability on a global scale[11]. This might be because assessing the trend and variability of global rice yield is limited due to insufficient information on rice management practices (e.g., planting method and timing, N fertilizer and manure, multiple-cropping systems) and the limited information to account for the management processes (e.g., flooded irrigation, planting method) within gridded global crop models[13].

Recent efforts have led to the development of a spatially explicit database on the seasonal distribution of global rice production, including planting and harvesting dates, nitrogen (N) fertilizer and manure application, and cropping intensity across rice-producing countries[14–17]. Building on this advancement, the present study aims to improve the modeled representation of key rice management practices, specifically, irrigation, N fertilizer, manure use, planting timing, and multiple-cropping systems, and to assess their contributions to global rice production from 1901 to 2015. In addition to these management drivers, we also evaluate the influence of time-varying environmental variables such as N deposition, atmospheric CO_2 concentrations, and climate change (i.e., changes in radiation, temperature, and precipitation).

To achieve this, we integrate the new spatial dataset on seasonal rice calendars and cropping intensity into a process-based land surface model, the Integrated Science Assessment Model for crops ($ISAM_{Crop_Rice}$). The version of $ISAM_{Crop_Rice}$ used in this study builds on previous developments for C_3 and C_4 crops (e.g., maize, soybean, and wheat) and bioenergy grasses (e.g., miscanthus, cave-in-rock, and alamo)[18–22]. It has been extended to better represent rice-specific growth dynamics.

The additional processes, which are critical for the rice productivity calculations, have been implemented in the model including (i) leaf area index (LAI) as the function of rice phenological development and time-varying specific leaf area (SLA) based on measurements; (ii) transplanting shock period to account for the effect of subsequent growth and development of transplanted rice, which is a conventional method to grow rice[23]; (iii) water surface energy budget and temperature under flooded irrigated conditions; and (iv) multiple rice growing seasons per year and application of time-varying N fertilizer and manure rates on rice growth. These additions are essential for improving rice productivity simulations and evaluating the relative importance of environmental and management factors. Ultimately, the study contributes to a better understanding of how specific, quantifiable interventions influence rice production over time and under changing environmental conditions.

Results

Model evaluation

Before addressing the study objectives using $ISAM_{Crop_Rice}$, we first evaluated the extent to which the model can respond to revised and newly implemented algorithms using various data sets. Using data from multiple site studies, we calibrated and evaluated the ISAM-estimated rice photosynthesis under different temperature conditions, C, water, and energy fluxes. The results show that calibrated $ISAM_{Crop_Rice}$ could capture seasonal patterns of LAI, canopy height, gross primary production, energy fluxes for flooded irrigated conditions, and soil and water temperature for the rice at various sites (Supplementary Result 1.1–1.4, Supplementary Fig. 17–22, Supplementary Tables 9–11).

The $ISAM_{Crop_Rice}$ estimated yield was evaluated using the data from eleven rice observation sites, including three micrometeorological tower sites (Supplementary Table 1), and at the country scale. Overall, the model-estimated yields across all sites show a good agreement with the field observations, with a *bias* of −0.54 t/ha (Fig. 1 and Supplementary Result 1.5). At the country scale, the model was able to capture FAO-reported rice production for 116 countries, averaged for 1961-2015[24] with Willmott's index[25] of 0.94 and a Pearson's correlation coefficient, R, of 0.99 (Fig. 2), except for Sub-Saharan African countries where modeled yield was somewhat overestimated (Supplementary Fig. 1). However, the yield overestimation in these countries had a limited effect on model estimated rice production (Supplementary Fig. 2) due to the relatively low rice harvested areas in these regions. Overall, the model captured about 83% of the production trend of FAO (Supplementary Fig. 3a), particularly after 2010, as well as FAO-reported detrended production annual variability (Supplementary Fig. 3b).

Global rice production and yield

Our estimated global rice production increased from 296 million tons in 1961 to 750 million tons in 2015 (Supplementary Fig. 3a), with a trend of 7.96 million tons/year, particularly in response to the expansion of the harvested area from 116 million hectares (hereafter ha) in 1961 to 162 million ha in 2015 (Supplementary Fig. 4a). During the same period, modeled yield increased by about 81% with a trend of 0.04 tons/ha/year (Supplementary Fig. 5) despite a decreasing precipitation trend of −0.26 mm/yr and an increasing temperature trend of 0.02 °C/yr (Supplementary Fig. 4g-h). It is because the negative climate impacts are alleviated by increasing multiple environmental and management variables over time (Supplementary Fig. 4a-f), including irrigated fraction (20%), atmospheric CO_2 concentration ($[CO_2]$) (26%), and N input through deposition (12%), fertilizer (73%), and manure (15%).

During 2006–2015, the estimated global production was 713 million tons (Fig. 3 and Supplementary Fig. 6a) and a yield of 4.43 tons/ha (Supplementary Fig. 5), harvested on a total of 161 million ha areas (Supplementary Fig. 6b). On the country scale, the world's top ten rice-producing countries accounted for 82% of total global production (Fig. 4a), with China, India, Thailand, Indonesia, and Bangladesh being the top five rice-producing countries, contributing 24%, 22%, 9%, 8%, and 5% of global rice production, respectively. While India was the second-largest producing country with the highest harvested area, its yield was the second lowest (3.53 tons/ha) among the top ten countries. China and the Philippines had the highest yield (5.84 tons/ha) and the lowest yield (3.16 tons/ha), respectively (Supplementary Fig. 7).

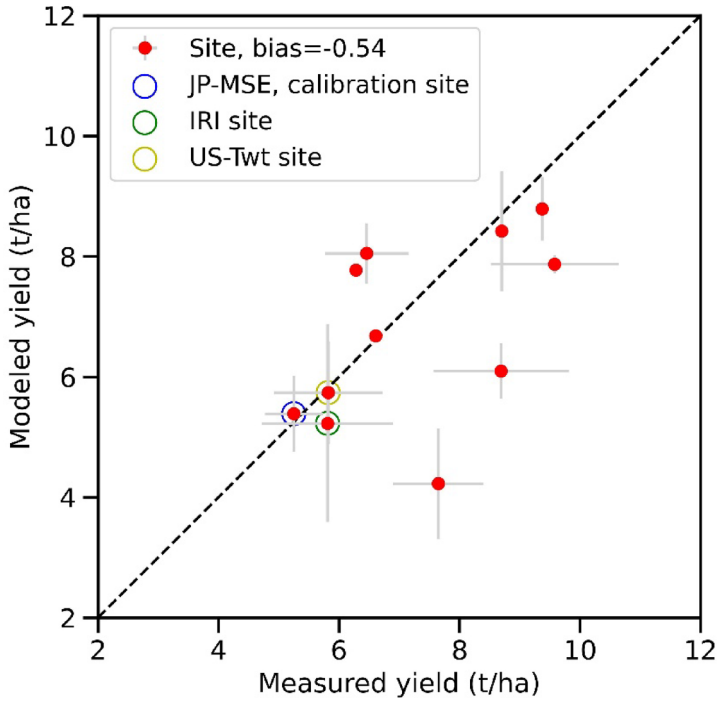


Fig. 1. Comparison between $ISAM_{Crop_Rice}$ modeled and measured yields for multiple sites. The model calibration and evaluation are performed over the periods of the available observation data, which vary from site to site. The main characteristics of the study sites are provided in Supplementary Table 1. The blue circle highlights the result of the calibrated site. The green and yellow circles highlight the results at the IRI and US-Twt sites. The gray lines indicate the one-standard-deviation range of yearly variability.

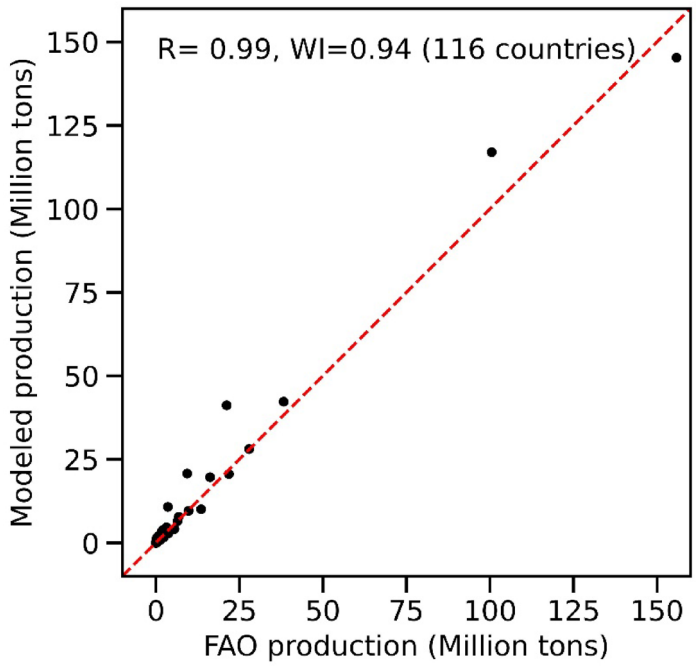


Fig. 2. Country-level rice production simulated by the ISAM model, averaged over 1961–2015. The x-axis shows the production data from FAO, and the y-axis shows the model simulation for 116 countries. *R* is Pearson's correlation, and the *WI* is the Willmott index.

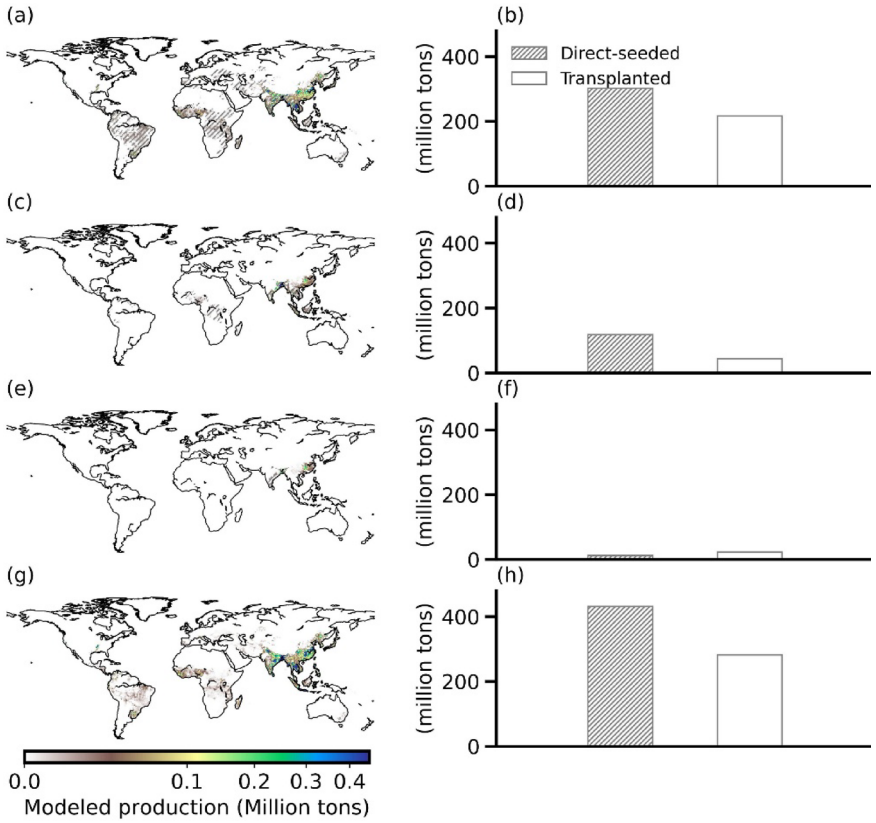


Fig. 3. Modeled rice production averaged for 2006–2015. Spatial plots are the distribution of production for **(a)** season one, **(c)** season two, **(e)** season three, and **(g)** the sum of the three seasons. Direct-seeded grids are hatched, and transplanted grids are w/o hatched in spatial plots **(a, c, and e)**. The bar plots **(b, d, f, h)** correspond to the modeled global total production of direct-seeded and transplanted rice. The custom code for the figure was written using Python (https://www.python.org/downloads/release/python-2718/. If inaccessible, see https://www.python.org/downloads/ and search for "Python 2.7.18").

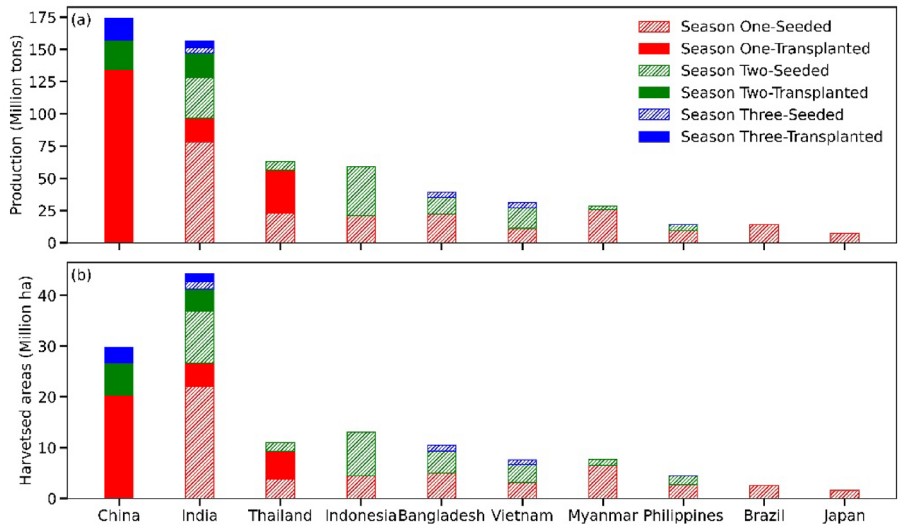


Fig. 4. **(a)** Estimated rice production and **(b)** harvested areas for the top-ten producing countries averaged for 2006–2015. The hatched segments in each bar show the direct-seeded rice production/areas for three seasons, whereas w/o hatched segments show transplanted rice production/areas.

The harvested area planted with the direct-seeded method indicated, in general, higher production than the transplanted method for 2006–2015 (Fig. 3), mainly because of the higher direct-seeded area. Of the global total harvested area, 67% was the direct-seeded area, and 33% was the transplanted area, which produced 431 and 282 million tons/yr of rice, or 60% and 40% of the global total production for 2006–2015. Despite the higher production, the yield for the seeded area of 4.0 tons/ha was 25% lower than the yield for the transplanted area (5.3 tons/ha) (Supplementary Fig. 8). In the top ten producing countries, China, India, and Thailand were the only countries that cultivated transplanted harvest areas, accounting for 19%, 7%, and 3% of the total harvested area, respectively (Fig. 4b). These countries accounted for the largest share of the world's population. Their higher demands for food were causing an increase in harvested areas. The estimated transplanted rice yields in these three countries were higher or the same compared to the direct-seeded yields (Supplementary Fig. 7). Although transplanted rice encountered transplanting shock (Supplementary Fig. 9), the results suggested that the lost yield was offset by the accumulation of more biomass during the reproductive period, mainly due to the longer growing period length, the favorable response for N fertilizer, and climate factors (Supplementary Fig. 10).

Global rice was cultivated in up to three distinct growing seasons within a calendar year, though not necessarily on the same plot of land. Some rice-producing regions, such as Bangladesh and Cambodia, practice triple cropping, while others, like China, follow single or double cropping systems. Rice is grown in double-cropped areas in early and late seasons, whereas single-cropped areas typically have a middle-season rice[14]. Season one accounts for the highest production (518 million tons or 73%), followed by season two (160 million tons or 22%) and season three (35 million tons or 5%).The seasonal production trend directly followed the trends in the seasonal harvested areas, decreasing with the season (109, 44, 8 million ha, or 68, 27, 5%) (Supplementary Fig. 6b). However, yields for three growing seasons (Supplementary Fig. 8) were not characterized by harvested area but by the variations of environmental factors and the length of growing season over three specific growing seasons (Supplementary Fig. 10). The season one yield for the global mean (Supplementary Fig. 11a) case was the highest (4.75 tons/ha) due to the most prolonged growing period; favorable environmental conditions, such as temperature and precipitation; and higher yield response to the N fertilizer applications (Supplementary Fig. 11b-e). In top-ten production countries, season one yield was the highest in China, Thailand, Indonesia, Bangladesh, Myanmar, and the Philippines (Supplementary Fig. 7). In contrast, although season two rice was grown with the lowest average global temperature during the growing season (Supplementary Fig. 11c) our analysis indicated the estimated yield was the lowest (3.64 tons/ha) among the three growing seasons due to lower N fertilizer rates than season three (Supplementary Fig. 11b) and the shortest growing period, and the lowest precipitation rates and incoming solar radiation (Supplementary Fig. 11d-f). On a regional scale, West Africa was the most impacted by unfavorable environmental and management conditions (Supplementary Fig. 10). This trend, in general, was also found in most of the top ten rice-producing countries (Supplementary Fig. 7). In season three, yield increased relative to season two in China due to the increasing length of the growing period with a weak positive temperature effect, suggesting an important role of lengthening the growing season to enhance photosynthetic activity, leaf area index, biomass accumulation, panicle development, and ultimately grain filling and yield. However, the response in India was just the opposite (Supplementary Fig. 7), mainly because of the unfavorable environmental and management conditions for growing rice (Supplementary Fig. 10). As a result, the average yield for India was almost 40% lower than China's yield. Overall, the global yield for season three (4.38 tons/ha) was higher than season two's (Supplementary Fig. 11a).

Regarding cropping intensity for 2006–2015, most of the top ten rice-producing countries harvested two-season rice (Fig. 4). Some locations in China can have either a single or a double-season rice, leading to three seasons in each grid cell. The countries that harvested rice for up to three seasons produced the most. These multiple harvested areas appeared in China, India, Bangladesh, Vietnam, and the Philippines, with 30, 44, 11, 8, and 5 million ha of areas devoted to rice harvests, which produced 24%, 22%, 5%, 4%, and 2% of global total rice production. Rice harvests in two seasons accounted for the 39 million ha and 21 million ha areas, with 25% and 11% of global production in the first and second harvest seasons, respectively, mainly in China, India, Africa, and Southeast Asia (Supplementary Fig. 6b). About 39 million ha of land was used to harvest single-season rice, contributing to 25% of global total production located in most of the growing regions, with the highest in the central parts of India.

Production responses to environmental and management changes

To study the contribution of environmental and management variables resulting from increased historical crop production, we conduct factorial model experiments, keeping one input driver fixed at the initial year (1900) conditions for simulations spanning 1901–2015, corresponding to the availability of climate data beginning in 1901. The results suggested that, except for climate change factors (e.g., precipitation and temperature), all environmental and management factors increased global rice production for 1961–2015 (Fig. 5). This period was selected to align with FAO-reported rice production data, which are available starting in 1961; historical gridded N fertilizer and manure data from GGCMI, which are available until 2015[16]; and RiceAtlas report[14] data for three rice growing seasons, which are not a time-series dataset but give a representative average condition in the early 21_{st} century via the collection of calendar practices between 2000 and 2015 (mostly 2010–2015). Climate change was the only factor that reduced global rice production. Among all the factors examined, management factors combined contributed to global changes in production by 76%, including irrigated harvested areas (39%), rainfed harvested areas (13%), and N fertilizer and manure (24%). The remaining 24% was attributed to environmental factors that included [CO_2] (30%), N deposition (1%), and climate change (−7%) for 2006–2015 (Supplementary Table 2 and Fig. 6).

The expansion of irrigated harvested areas significantly contributed to the increase in global rice production, partly due to the greater availability and use of agricultural inputs (e.g., chemical fertilizers and pesticides)

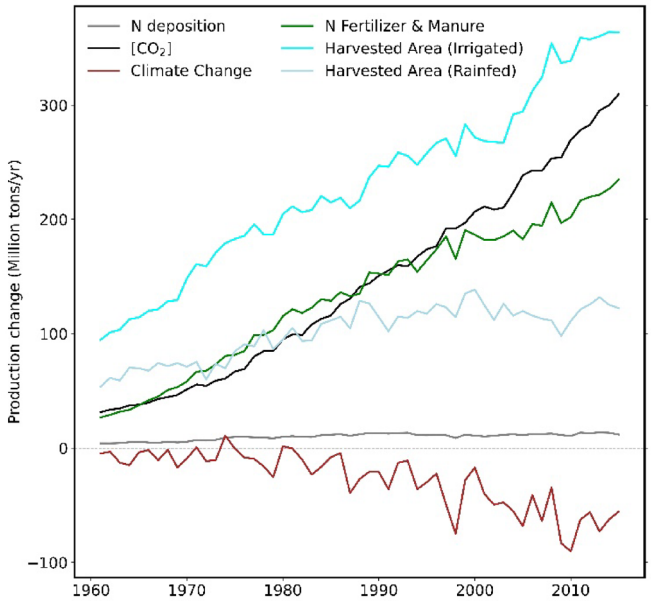


Fig. 5. Estimated yearly global rice production changes due to various environmental and management factors for 1961–2015.

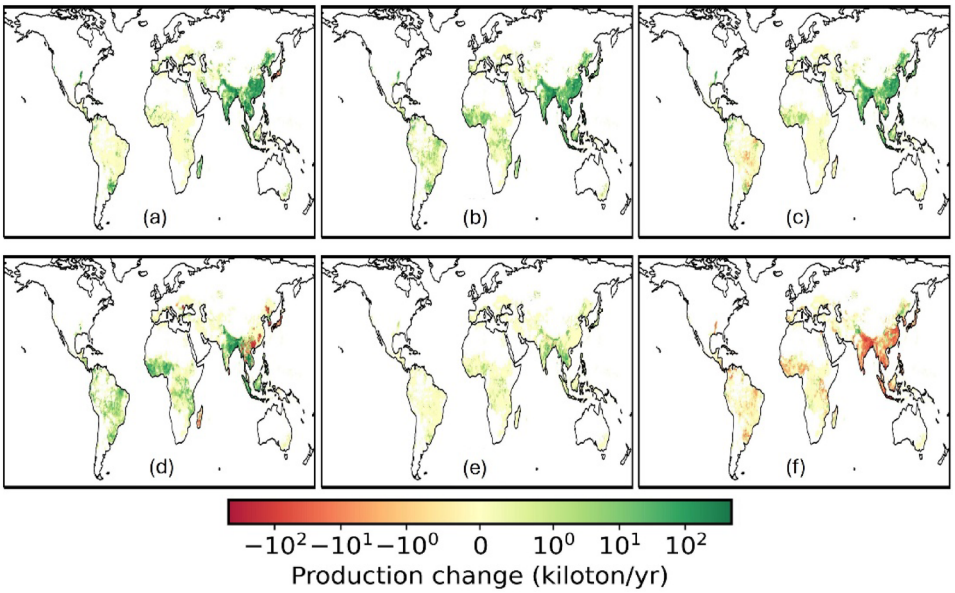


Fig. 6. Changes in yearly global rice production due to various environmental and management factors averaged for 2006–2015 at 0.5-degree resolution. Positive values indicate that the effect increases production, and negative values indicate that the effect reduces production. **(a)** harvested irrigated area, **(b)** [CO_2], **(c)** N fertilizer and manure, **(d)** harvested rainfed area, **(e)** N deposition, and **(f)** climate change. The color bar legend shows a logarithmic scale. The custom code for the figure was written using Python (https://www.python.org/downloads/release/python-2718/. If inaccessible, see https://www.python.org/downloads/ and search for "Python 2.7.18").

and more intensive human management typically associated with irrigated systems[26,27]. Regions such as South Asia, Southeast Asia, and East Asia experienced notable growth in irrigated area and correspondingly high rice production during 2006–2015 (Fig. 6a). Out of 347 million tons of global production increased per year (Supplementary Table 2), China produced the greatest amount (30%), followed by India (20%) and Thailand (10%).

Rising CO_2 concentration was the second most important environmental contribution factor, increasing global rice production by 273 million tons annually from 2006 to 2015 (Fig. 6b and Supplementary Table 2). China and India contributed 24% each to this total, followed by Indonesia at 9%.

The intensified application of fertilizer and manure continued to increase rice production with time, resulting in an increase of 212 million tons per year in global production (Fig. 6c and Supplementary Table 2) from 2006 to 2015. N fertilization from manure and fertilizer led to global production changes in China (29%), followed by India (26%) and Indonesia (11%). In some countries with N fertilizer and manure application, such as Brazil, the N application lowered production. This was attributed to the relatively lower N application rate and higher precipitation rates during 2006–2015, resulting in lower N supply and higher N losses due to leaching and denitrification.

While rice production also increased in the harvested rainfed areas, much less than in the irrigated areas, contributing 118 million tons of change per year (Fig. 6d and Supplementary Table 2). The three top-ten rice-producing countries that saw higher production were India (50%), Thailand (16%), and Indonesia (20%). But China, Myanmar, and Japan saw decreased production due to reduced rainfed harvested areas.

Nitrogen deposition led to the lowest positive effect among all factors, contributing about 13 million tons per year, particularly in South Asia and Mainland Southeast Asia (Fig. 6e and Supplementary Table 2).

Climate change, associated with increasing temperature and decreasing precipitation, decreased global rice production (Fig. 6f and Supplementary Table 2). For 2006–2015, climate change reduced 62 million tons of the worldwide output per year, with the highest reduction in India (30%), particularly in the central and east Indo-Gangetic Plain (Fig. 6f), followed by Indonesia (15%) and China (14%).

It is important to note that the interaction between environmental and management factors can produce interactive effects, and the outcome can be nonlinear. To examine the relative importance of interactive effects versus direct effects of the individual factors, we also calculated the direct effect of individual factors on rice production (see the method section). Our simulation results suggest that the interaction of various factors changes non-linearity over time and plays a significant role in rice production compared to the direct effects of individual factors over time, highlighting that production increase due to N input and CO_2 occurs concurrently with the expanding irrigated and rainfed harvested areas that further enhance global rice production in the interactive case (Fig. 5) compared to the direct case (Supplementary Fig. 23).

Discussion

Our study shows that rice production has steadily increased since the 1960s, given the expansion of rice cultivation under a changing climate and positive responses of environmental factors, N deposition, elevated carbon dioxide, and land-management practices, including nitrogen fertilizer and manure application and irrigation. Farmers often apply excessive amounts of N fertilizer without fully understanding the consequences in pursuit of stable and high yields. This practice leads to various issues, including environmental pollution, energy inefficiency, soil degradation, and reduced production efficiency[28]. Despite higher fertilizer application rates, our study also shows that global rice production growth decelerated from 2.6% in the 1960s to 1.3% in 2006–2015. It is because land fertility and water availability are declining, even though irrigation and N fertilizer application rates have been increasing since the 1960s. Several studies[29,30] have shown that in recent decades these inputs could not fully offset the negative effects of reduced water resources and soil degradation, contributing to a slowdown in rice yield growth across major producing regions. To address these challenges, recent studies have identified potential management practices that can improve crop yields while cost-effectively reducing N-related pollution at the field scale and enhancing agroecosystem sustainability[30,31].

Multiple cropping increases overall production in some Southeast Asian countries, such as Bangladesh and Cambodia. Rice sown in season one produces the highest yield due to the most prolonged growing period and favorable temperature and precipitation conditions, but productivity drops during the later growing seasons due to short-duration varieties.

While direct-seeded rice cultivation has many advantages, such as decreasing water consumption, reducing labor requirements, and increasing resource-use efficiency[32], our results indicate that global transplanted rice yields are higher than those of direct-seeded rice due to management practices that include longer growing seasons, cooler temperatures, and higher N fertilizer application. Our study shows that the overall global yield from direct-seeded was 25% lower than that of transplanting. The meta-analysis results support our study finding[33], which pointed out the direct-seeded yield is 12% lower than that of transplanting. Still, results are highly variable (−2% and − 42%), depending on management practices, soil type, and climate conditions.

Our results indicated that the impact of CO_2 fertilization on rice yield shows substantial regional and seasonal variation (Supplementary Fig. 24), largely driven by differences in local environmental conditions and agricultural management practices. Specifically, the CO_2 fertilization effect on rice yield was found to be: (1) positively correlated with nitrogen fertilizer application ($r = 0.28$, $P < 0.001$); (2) negatively correlated with accumulated precipitation during the growing period ($r = -0.13$, $P < 0.001$); (3) negatively correlated with maximum LAI during the growing period ($r = -0.43$, $P < 0.001$); and (4) negatively correlated with the length of the growing period ($r = -0.38$, $P < 0.001$). These relationships are consistent with known physiological mechanisms. Increased nitrogen availability can alleviate CO_2-induced photosynthetic downregulation caused by nitrogen limitation[18,34]. Elevated CO_2 reduces stomatal conductance, increasing soil moisture availability, which diminishes the relative importance of precipitation[18,34,35]. The photosynthetic enhancement from elevated CO_2 is generally stronger under low LAI conditions due to reduced intra-canopy shading[18,35]. Furthermore, a longer growing period tends to increase the maximum LAI ($r = 0.49$, $P < 0.001$), reducing the crop's responsiveness to elevated CO_2 due to self-shading and reduced marginal gains in photosynthetic efficiency.

Warming temperatures resulted in a 7% global rice yield loss and a yield reduction of −3.5% to −14.1% in the top ten producing countries during 2006–2015 (Supplementary Table 3). This loss is primarily due to a shortened

growing season, increased heat stress during the reproductive period[36], temperature stress on photosynthesis rates, water vapor deficit, and droughts. From 1901 to 2015, the average temperature over rice fields increased by about 1.5 °C, from 24.6 °C to 26.1 °C, leading to a 5.3% yield loss per degree Celsius. Our estimates align with previous findings of a −3.2 ± 3.7% yield loss per degree Celsius, based on an integrated study using global grid-based and local models, statistical regressions, and field-warming experiments[37]. This study uses a model-data integrated approach, which considers some of the important processes critical for rice yield and its synergy with environment and management variables, including surface water storage, flooded irrigation, multiple growing seasons with two planting methods, transplanted and direct-seeded planting, on a global scale. We compare our data-modeling framework with the results of other existing products. The modeled productions for ca. 2010 (average for 2009–2011) indicated that our study approach captured SPAM2010v1[38] data with Willmott's index[25] of 0.88 and a correlation coefficient of 0.91 at the gridded level. The modeled global rice production was 699 million tons, close to 703 million tons from SPAM2010v1. The modeled production along the latitudinal gradients for ca. 2010 was also compared well with SPAM2010v1 data. The production peaked in the tropics (10°S–30°N) because of the large harvested area (Supplementary Fig. 12), followed by northern middle latitudes (30°N–45°N) and southern middle latitudes (30°S). Compared to RiceAtlas[14], which reported seasonal rice production of 714 million tons for 2010–2012, our results were 727 million tons (Supplementary Table 4). Comparing the estimates for planting methods, the estimates were about 9% higher than RiceAltas in transplanted rice production but slightly lower (3%) than those of direct-seeded. Our study results for rice production were somewhat higher in season one but marginally lower in season two than RiceAtlas. However, our study results of rice production for season three using the direct-seeded planting method were consistent with RiceAtlas but lower than those for the transplanted method.

Our sensitivity analysis at multiple sites indicates that variables and parameters (Supplementary Table 9) associated with management practices and photosynthesis play essential roles in modulating simulated rice yield (Supplementary Fig. 13 and Supplementary Result 1.6). However, due to limited data worldwide, model parameters like seeding rate and the fraction of residue removal are constantly prescribed in global simulations. More efforts to implement additional processes and spatial and temporal patterns of management data sets could help reduce uncertainties and better characterize rice growth in models.

Given the importance of rice yield projection under climate change and the corresponding biophysical and biogeochemical effects on climate, there is a pressing need for additional modeling implementation of management practices that can affect rice production and climate projection through crop-climate interactions. Our modeling framework captures the overall observed production trend (Supplemental Fig. 3), though there is some bias and overestimation of production due to limited data availability for many variables prior to 2006. For instance, most management practices and cultivars are based on data from 2006 to 2015. Before this period, we assumed that changes in cultivars, seeding rates, multiple cropping systems, seedling ages, and planting times remained constant due to a lack of global data. Additionally, we have not accounted for other technological factors, such as labor and machinery availability, crop protection, weed management, pesticide use, and genetically improved cultivars, due to insufficient data on technological development. Despite some data and model process limitations, our process-based data-modeling study provides bottom-up global estimates of spatial and temporal distributions of rice yield with possible management practices in detail. These include transplanting, surface water storage, flooded irrigation, time-varying management inputs (N and harvested areas), and three rice-growing seasons. Our spatial and temporal analysis has identified the relative importance of various environmental and management factors influencing rice productivity at the grid level, which provides insight into regional-scale challenges and opportunities. These spatially explicit results also provide a foundation for informing future adaptation strategies tailored to local conditions.

Conclusion

Overall, this study presents a global, process-based analysis of historical rice production that explicitly accounts for changing climate, environmental conditions, and time-varying management practices. We show that global rice production has increased steadily since the 1960s, driven by the expansion of harvested areas, irrigation, nitrogen inputs, and rising atmospheric CO_2, which has partly compensated for the negative effects of warming. However, the rate of production growth slowed over time, indicating that increasing external inputs cannot indefinitely offset the decline in land fertility and water limitations.

Our results further demonstrate that rice productivity is strongly controlled by management and production systems. Multiple cropping enhanced production in parts of Southeast Asia; transplanted rice outperformed direct-seeded rice globally; and the CO_2 fertilization effect varied substantially with nitrogen availability, precipitation, canopy structure, and growing-season length. Warming caused notable yield losses, primarily through shortened crop duration, heat stress, and increased water stress. These findings highlight that historical rice production trends arise from strong interactions among climate, environmental conditions, and agricultural management.

The robustness of these results is supported by model calibration and evaluation against site-level observations, including leaf area index, biomass, carbon, water, and energy fluxes, and rice yield across multiple experimental and flux tower sites, as well as comparisons with independent global production datasets. These evaluations indicate that the model framework can capture both site-level processes and large-scale production patterns.

Despite these strengths, several limitations remain. Global simulations are constrained by the limited availability of long-term, spatially explicit data on management practices, including cultivar changes, seeding rates, residue management, and planting schedules, particularly prior to 2006. In addition, important technological and socio-economic factors, such as mechanization, crop protection, pesticide use, and genetic improvements, are not explicitly represented due to data limitations. These constraints introduce uncertainty in attributing changes in rice production to individual drivers.

Future work should focus on improving the representation of management practices by leveraging better spatial and temporal datasets, refining key model parameters and processes with additional observations, and incorporating technological and socio-economic drivers that influence agricultural systems. Extending this framework to future climate scenarios and applying it to region-specific adaptation assessments will further enhance its utility for projecting rice production and supporting sustainable agricultural planning under changing environmental conditions.

Methods

Model overview

The ISAM model used here to study rice growth processes is a coupled biophysical and biogeochemical cycle model with 0.5° × 0.5° spatial and multitemporal resolution from half-hour to the year for different processes[39–44]. Energy and water fluxes are calculated using coupled leaf/canopy photosynthesis, surface energy, and hydrological processes[43,45]. Soil input data prescribed in ISAM was derived from the Harmonized World Soil Database (HWSD)[16]. ISAM consists of prognostic and coupled C and N processes associated with residue and litter decomposition changes[44,46], soil organic matter (SOM), and soil N processes, including N deposition, fixation, mineralization, immobilization, nitrification, denitrification, volatilization, and leaching[41,47]. C assimilation is allocated to vegetation organs and transferred to litter and SOM pools. The modeled C and N cycles account for feedback processes from environmental variables such as [CO_2], climate change and variability (e.g., radiation, temperature, precipitation), N deposition, and management practices such as irrigation, N manure, and fertilizer application[18,47,48].

The standard version of the ISAM that simulated natural vegetation and generic crops[41,49–51] had been extended to represent dynamical processes for major arable crops and bioenergy crops[18–22]. The dynamical crop growth component of ISAM includes vital processes such as crop dynamic phenological development, structure growth (e.g., LAI, canopy height, and root depth and distribution), biomass accumulation, and allocation in different organs. The crop phenology is determined by accumulated crop-specific growing degree-days (GDDs) and heat unit index[19,48]. The planting time is either prescribed based on data or determined by environmental conditions[18,19,48]. Assimilated C is allocated to different tissues depending on accumulated heat and resource availability, including light, water, and N. Heat stress is implemented to consider the detrimental effects of high temperatures on grains during the reproductive stage of the phenology[18,48]. ISAM has been applied to various model intercomparison agricultural studies[16,20,47](See also Supplementary Result Sect. 1.7).

Extended version of rice in ISAM

Here we implement rice-specific processes into ISAM. Since rice is a C3 crop, the C3 crops of ISAM framework ($ISAM_{Crop_C3}$), which also has been used to calculate the productivity of other C3 crops, for example, wheat[48] and soybean[18,19], is the foundation for implementing rice growth processes into ISAM. The ISAM rice model framework (hereafter $ISAM_{Crop_Rice}$) is shown in Supplementary Fig. 14. $ISAM_{Crop_C3}$ equations are available in previous studies[19,48]. The various equations and parameter values specific to the variables appearing in these equations, some of which are based on published studies and others model calibration, as well as the definition of variables used in the equations, are listed in Supplementary Tables 5, 6, and 7. Next, we describe the processes that are newly added to $ISAM_{Crop_Rice}$.

The newly added process to $ISAM_{Crop_Rice}$

Implementation of multiple growing season phenology

We consider the maximum of three rice growing seasons per year in each grid cell (Supplementary Method 1). Following the RiceAtlas report[14], rice is modeled using two planting methods (direct-seeded or transplanted) for all seasons. In $ISAM_{Crop_C3}$, crop seeds with an initial carbon mass are directly sown at the planting time, followed by five growth periods, starting with the emergence period. In $ISAM_{Crop_Rice}$ the crop growth phenology for the transplanted method in each growing season has been partitioned into six stages rather than five, as considered in $ISAM_{Crop_C3}$ (Supplementary Method 2 and Supplementary Fig. 14a). For determining the harvesting date, we follow the method of AgMIP[16](Supplementary Method 3). We assume the maximum growing season length of 240 days[52]. The maximum length of each phenological period, including the fraction of accumulated heat units and accumulated maximum days, is determined using Mase paddy flux site in Japan (JP-MSE[53] data for phenological periods and calibrated LAI values, which are discussed next.

Leaf area development

LAI is estimated by multiplying leaf carbon mass by specific leaf area (SLA), defined as a ratio of leaf area to leaf biomass, which varies with time in each phenological period (Supplementary Fig. 15), rather than assuming fixed value over the entire growing season, which is considered in $ISAM_{Crop_C3}$ (Supplementary Method 4).

Accounting for flooded irrigation conditions

ISAM accounts for irrigation processes to alleviate water stress conditions for various crops[18,48]. In $ISAM_{Crop_Rice}$, we extend this scheme by accounting for the flooded irrigation associated with the surface water layer over paddy fields. In flooded irrigation, the surface water layer depth (H_w) increases above the ground up to the water layer target height (H_{wmax}). The flooded irrigation is applied during the rice-growing period if H_w is below H_{wmax} after the transplanting shock period in the transplanting method or the emergence period in the directseeded method (Supplementary Method 5.1). If there is a precipitation event after H_w reaches the H_{wmax}, the excess precipitation is lost as surface runoff. Flooded surface water layer temperature over rice paddies modulates the ground temperature and surface energy budgets via changes in the surface properties and the energy fluxes. Therefore, the model calculates the temperature of the flooded surface water layer (Supplementary Method 5.2).

The surface water is drained before the harvest stage of the phenology, and thereafter, the surface hydrological processes calculations follow $ISAM_{Crop_C3}$.

Global model experimental design and analysis

First, we spin up $ISAM_{Crop_Rice}$ by recycling climate forcing data with temporally fixed [CO_2], land cover, N deposition, manure, and fertilizer at the 1900 level. We recycle CRU JRA[54,55] climate forcing between 1901 and 1920 for the spin-up process, since climate data before 1901 is unavailable. The spin-up process allows model soil moisture, temperature, C, and N to reach a steady state. Next, we perform model simulation for multiple rice-growing seasons from 1901 to 2015 by prescribing temporally varied climate, [CO_2], and N inputs (i.e., deposition, manure, and fertilizer) (Supplementary Table 8). Six additional simulations are conducted to determine the historical effects of environmental changes and management options, each using the same configuration and forcings as for E_{Ref} but with one of the six factors remaining fixed at the spin-up (1900) conditions in each experiment, allowing for interactions among the five changing factors but not with the fixed one. These simulations are performed to study the effects of climate change (E_{Cli}), [CO_2] (E_{CO2}), N deposition (E_{Ndep}), N fertilizer and manure application (E_{Nin}), rainfed harvested area conversion (E_{Rai}), and irrigated harvested area conversion (E_{Irr}). These experiments allowed for no interactive effect of each factor on the others. We then estimate the effect of each factor by differencing the yields and production between the E_{Ref} and one of the six simulations. This method allows us to isolate the impact of individual factors while still accounting for potential interactions.

To quantify the contribution of interactive effects, we conducted six additional simulations. In each simulation, one time-dependent input factor was varied. In contrast, the remaining five factors were held constant at their spin-up values, thereby eliminating interactions between the varying factor and the others. By comparing each of these simulations to the spin-up experiment, in which all factors were held constant, we estimated the direct effect of each individual factor. The contribution of interactions for each factor was quantified by comparing simulation results with interactive effects to those without.

The irrigated and rainfed rice in each model grid is treated as separate plant functional types with different soil columns. So, there is no transfer of irrigated land water to rainfed land. The rice yield for each grid cell is irrigated- and rainfed-weighted yield by harvested areas. At harvest, rice yield is converted from the dry grain carbon pool, with the assumption of 45% carbon in the dry matter[56] and the average water content of 13% in rice[57]. Rice yield is presented at 0.5° x 0.5° grids and aggregated to national and global scales. Production was represented by multiplying harvested areas in hectares by the yield in tons/hectare.

The cropland area of each grid cell is discretized into irrigated and rainfed areas. The irrigated fractional area for each grid cell for 1900–2015 is calculated using various data sets. The method to calculate the fractions is described in Supplementary Method 6.1. The method to produce the temporal trends and spatial distributions of harvested areas for three rice growing seasons over rainfed and irrigated systems for the period 1900–2015 is described in Supplementary Method 6.2.

Environment and management forcing data sources

Seven climate variables are used as model input, including near-surface specific humidity, wind speed, air pressure, and temperature, precipitation, surface downwelling longwave, and shortwave radiation. The data used in this study is from CRU JRA[54,55]. Annual [CO_2] data is taken from the Global Carbon Budget[58]. Monthly N deposition data is obtained from NCAR Chemistry-Climate Model Initiative (CCMI) results[59], which accounts for N sources from biomass burning, soils, and all sources of fossil fuels, including fossil fuel use in mining, manufacturing, and transportation of N fertilizer. N deposition in the model applies at the weekly scale. Gridded N fertilizer and manure data for 1900–2015 are applied using phase 3 of the Global Gridded Crop Model Intercomparison (GGCMI)[15] data. The nitrogen (N) application rates from mineral fertilizers are derived from harmonized, spatially and temporally explicit datasets. These datasets capture inter-annual variation at both national and global scales, primarily driven by modeled land use. Although they do not explicitly represent farmer-level behavioral variability, such as decisions influenced by weather, credit access, or local extension services, the model accounts for the effects of fertilizer applied in previous years on soil mineral nitrogen and its influence on rice yield. This is achieved through the dynamic nitrogen processes incorporated in the ISAM model, including fixation, mineralization, immobilization, leaching, nitrification, uptake, volatilization, and denitrification. We assume the N fertilizer and manure rates for each rice-growing season are the same but vary annually.

Model calibration and evaluation

We use the data from the Mase paddy flux site in Japan, JP-MSE, (Supplementary Table 1) to calibrate $ISAM_{Crop_Rice}$ because it provides well-documented rice data for LAI, canopy height, biomass, and management information, including transplanting date, harvest time, and water level for rice growing seasons between 2002 and 2006. Sowing dates are set 20 days ahead of transplanting dates at this location[53]. We evaluate the modeled LAI and biomass using the IRRI Flux Research Site (IRI) for 2009, 2010, and 2012–2014. The data collected at the IRI site is available for two growing seasons (dry/wet) per year. We calibrate the C, energy, and water fluxes using JP-MSE site data and evaluate these fluxes using IRI and one additional eddy flux tower site, the Twitchell Island (US-Twt) for 2010–2014. We evaluate modeled rice yield using three flux site data, JP-MSE, IRI, US-Twt, and eight additional published studies' data (Supplementary Table 1). We also calibrate the simulated leaf photosynthesis and its temperature response using the data from an experimental site[34]. This enhances the model's capability to simulate the relationships between rice photosynthesis rates and environmental conditions that are compared well with the observations (Supplementary Method 7 and Supplementary Fig. 16). The compiles site-specific environmental and management data, including N fertilizer amount and timing, planting

and harvest times, seedling age, and seeding density, and the model calibration and evaluation methods are further described in Supplementary Method 8.

Selection of period 2006–2015

We select this period to compare the model results with the observation data. The 2006–2015 period selection provides a reliable baseline for comparing historical and future scenarios. This decade offers the most comprehensive and consistent observational data on rice production and key ecosystem variables, such as biomass, gross primary production, LAI, and yield, essential for calibrating and validating model parameters. This, in turn, enhances the robustness of long-term historical and future projections and supports evaluating management practices at broader spatial and temporal scales.

Data availability

The rice yield and production results for three seasons, averaged over 2006-2015, along with all codes for plotting figures and the corresponding raw data in the main text, can be downloaded from the ISAM website ([http://climate.atmos.uiuc.edu/rice_data]). The site also contains a READ_ME file that describes the raw dataset structure, explains each file, and documents how the raw data and scripts are used to generate the figures. All datasets used in this study are publicly available, including flux tower sites data from AsiaFlux ([https://asiaflux.net/]) and AmeriFlux ([https://ameriflux.lbl.gov/]), FAO production data ([https://www.fao.org/faostat/en/#home]), RiceAtlas data ([https://dataverse.harvard.edu/dataset.xhtml?persistentId=doi:10.7910/DVN/JE6R2R]), and SPAM data ([https://dataverse.harvard.edu/dataset.xhtml?persistentId=doi:10.7910/DVN/PRFF8V]). All other results presented in the paper and Supplementary Information sections are available from the corresponding author upon request.

Code availability

The corresponding author can request details and codes for the rice model used in this study.

Received: 7 January 2025; Accepted: 28 May 2026
Published online: 03 June 2026

References

1. Muthayya, S., Sugimoto, J. D., Montgomery, S. & Maberly, G. F. An overview of global rice production, supply, trade, and consumption. *Ann. N Y Acad. Sci.* **1324**, 7–14 (2014).
2. Horie, T. et al. Can yields of lowland rice resume the increases that they showed in the 1980s?. *Plant Prod. Sci.* **8**, 259–274 (2005).
3. Ray, D. K., Ramankutty, N., Mueller, N. D., West, P. C. & Foley, J. A. Recent patterns of crop yield growth and stagnation. *Nat. Commun.* **3**, 1293–1297 (2012).
4. Bouman, B. A. M., Humphreys, E., Tuong, T. P. & Barker, R. *Rice and Water. Advances in Agronomy 92* (Elsevier Masson SAS, 2007).
5. Zhao, C. et al. Plausible rice yield losses under future climate warming. *Nat. Plants.* **3**, 1–5 (2016).
6. Masutomi, Y., Ono, K., Mano, M., Maruyama, A. & Miyata, A. A land surface model combined with a crop growth model for paddy rice (MATCRO-Rice v. 1) - Part 1: Model description. *Geosci. Model. Dev.* https://doi.org/10.5194/gmd-9-4133-2016 (2016).
7. Maruyama, A. & Kuwagata, T. Coupling land surface and crop growth models to estimate the effects of changes in the growing season on energy balance and water use of rice paddies. *Agric. For. Meteorol.* **150**, 919–930 (2010).
8. Wang, X. et al. Management outweighs climate change on affecting length of rice growing period for early rice and single rice in China during 1991–2012. *Agric. For. Meteorol.* **233**, 1–11 (2017).
9. Huang, Y. et al. BESS-Rice: A remote sensing derived and biophysical process-based rice productivity simulation model. *Agric. For. Meteorol.* **256–257**, 253–269 (2018).
10. Li, T. et al. Uncertainties in predicting rice yield by current crop models under a wide range of climatic conditions. *Glob. Chang. Biol.* **21**, 1328–1341 (2015).
11. Müller, C. et al. Global gridded crop model evaluation: Benchmarking, skills, deficiencies and implications. *Geosci. Model Dev.* https://doi.org/10.5194/gmd-10-1403-2017 (2017).
12. Elliott, J. et al. The global gridded crop model intercomparison: Data and modeling protocols for Phase 1 (v1.0). *Geosci. Model Dev.* **8**, 261–277 (2015).
13. Iizumi, T. & Ramankutty, N. How do weather and climate influence cropping area and intensity?. *Glob. Food Secur.* **4**, 46–50 (2015).
14. Laborte, A. G. et al. RiceAtlas, a spatial database of global rice calendars and production. *Sci. Data.* https://doi.org/10.1038/sdata.2017.74 (2017).
15. Heinke, J., Müller, C., Mueller, N. D. & Jägermeyr, J. N application rates from mineral fertiliser and manure (1.0) [Data set]. Zenodo. (2021). Available at: https://doi.org/10.5281/zenodo.4954582
16. Jägermeyr, J. et al. Climate impacts on global agriculture emerge earlier in new generation of climate and crop models. *Nat. Food.* **2**, 873–885 (2021).
17. Lin, T. S. & Jain, A. K. Assessment of Climate Change Impact on Rice Production Over South and Southeast Asia Under CMIP6 Climate Scenarios. *In: Vadrevu, K.P., Le Toan, T., Ray, S.S., Justice, C. (eds) Remote Sensing of Agriculture and Land Cover/Land Use Changes in South and Southeast Asian Countries. Springer, Cham.* (2022). https://doi.org/10.1007/978-3-030-92365-5_21
18. Lin, T. S., Song, Y., Lawrence, P., Kheshgi, H. S. & Jain, A. K. Worldwide maize and soybean yield response to environmental and management factors over the 20th and 21st centuries. *J. Geophys. Res. Biogeosciences* **126**, 006304 (2021).
19. Song, Y., Jain, A. K. & McIsaac, G. F. Implementation of dynamic crop growth processes into a land surface model: Evaluation of energy, water and carbon fluxes under corn and soybean rotation. *Biogeosciences* **10**, 8039–8066 (2013).
20. Niyogi, D. et al. Crop models capture the impacts of climate variability on corn yield. *Geophys. Res. Lett.* https://doi.org/10.1002/2015GL063841 (2015).
21. Song, Y., Jain, A. K., Landuyt, W., Kheshgi, H. S. & Khanna, M. Estimates of biomass yield for perennial bioenergy grasses in the USA. *Bioenergy Res.* **8**, 688–715 (2015).
22. Song, Y. et al. The interplay between bioenergy grass production and water resources in the United States of America. *Environ. Sci. Technol.* **50**, 3010–3019 (2016).
23. Chakraborty, D. et al. A global analysis of alternative tillage and crop establishment practices for economically and environmentally efficient rice production. *Sci. Rep.* **7**, 1–11 (2017).
24. FAOSTAT (Food and Agriculture Organization of the United Nations). (2021).

25. Willmott, C. J., Robeson, S. M. & Matsuura, K. A refined index of model performance. *Int. J. Climatol.* **32**, 2088–2094 (2012).
26. Cassman, K. G. Ecological intensification of cereal production systems: Yield potential, soil quality, and precision agriculture. *Proc. Natl. Acad. Sci. U. S. A.* **96**, 5952–5959. https://doi.org/10.1073/pnas.96.11.5952 (1999).
27. Ladha, J. K., Dawe, D., Pathak, H., Padre, A. T., Yadav, R. L., Singh, B., … Yadvinder-Singh.How extensive are yield declines in long-term rice-wheat experiments in Asia? Field Crops Research, 81(2–3), 159–180 (2003). https://doi.org/10.1016/S0378-4290(02)00219-8.
28. Jain, A. K. Greenhouse gas emissions from nitrogen fertilizers. *Nat. food.* **4**, 139–140 (2023).
29. Ray, D. et al. Recent patterns of crop yield growth and stagnation. *Nat. Commun.* **3**, 1293. https://doi.org/10.1038/ncomms2296 (2012).
30. Zhang, X. et al. Managing nitrogen for sustainable development. *Nature* **528**, 51–59 (2015).
31. Waqas, M., Hawkesford, M. J. & Geilfus, C. M. Feeding the world sustainably: efficient nitrogen use. *Trends Plant Sci.* **28**, 505–508 (2023).
32. Panda, S. et al. Proofing direct-seeded rice with better root plasticity and architecture. *Int. J. Mol. Sci.* **22**, 1–33 (2021).
33. Xu, L., Li, X., Wang, X., Xiong, D. & Wang, F. Comparing the grain yields of direct-seeded and transplanted rice: A meta-analysis. *Agronomy*. **9**(11), 767 (2019).
34. Borjigidai, A. et al. Seasonal changes in temperature dependence of photosynthetic rate in rice under a free-air CO2 enrichment. *Ann. Bot.* **97**, 549–557 (2006).
35. Sakurai, G., Iizumi, T., Nishimori, M. & Yokozawa, M. How much has the increase in atmospheric CO2 directly affected past soybean production. *Sci. Rep.* **4**, 4978 (2015).
36. Teixeira, E. I., Fischer, G., van Velthuizen, H., Walter, C. & Ewert, F. Global hot-spots of heat stress on agricultural crops due to climate change. *Agric. For. Meteorol.* **170**, 206–215 (2013).
37. Zhao, C. et al. Temperature increase reduces global yields of major crops in four independent estimates. *Proc. Natl. Acad. Sci.* **114** (35), 9326–9331. https://doi.org/10.1073/pnas.1701762114 (2017).
38. Yu, Q. et al. A cultivated planet in 2010-Part 2: The global gridded agricultural-production maps. *Earth Syst. Sci. Data*. **12**, 3545–3572 (2020).
39. Jain, A. K., Meiyappan, P., Song, Y. & House, J. I. CO2 emissions from land-use change affected more by nitrogen cycle, than by the choice of land-cover data. *Glob Chang. Biol.* **19**, 2893–2906 (2013).
40. Jain, A. et al. Nitrogen attenuation of terrestrial carbon cycle response to global environmental factors. *Global Biogeochem. Cycles* **23**, n/a-n/a (2009).
41. Yang, X., Wittig, V., Jain, A. K. & Post, W. Integration of nitrogen cycle dynamics into the Integrated Science Assessment Model for the study of terrestrial ecosystem responses to global change. *Global Biogeochem. Cycles*. **23**, 1–18 (2009).
42. El-Masri, B. et al. Carbon dynamics in the Amazonian Basin: Integration of eddy covariance and ecophysiological data with a land surface model. *Agric. Meteorol.* https://doi.org/10.1016/j.agrformet.2013.03.011 (2013).
43. Barman, R., Jain, A. K. & Liang, M. Climate-driven uncertainties in modeling terrestrial gross primary production: A site level to global-scale analysis. *Glob Chang. Biol.* **20**, 1394–1411 (2014).
44. Shu, S., Jain, A. K., Koven, C. D. & Mishra, U. Estimation of Permafrost SOC Stock and Turnover Time Using a Land Surface Model With Vertical Heterogeneity of Permafrost Soils. *Global Biogeochem. Cycles*. https://doi.org/10.1029/2020GB006585 (2020).
45. Barman, R., Jain, A. K. & Liang, M. Climate-driven uncertainties in modeling terrestrial energy and water fluxes: A site-level to global-scale analysis. *Glob Chang. Biol.* https://doi.org/10.1111/gcb.12473 (2014).
46. Shu, S., Jain, A. K. & Kheshgi, H. S. Investigating Wetland and Nonwetland Soil Methane Emissions and Sinks Across the Contiguous United States Using a Land Surface Model. *Global Biogeochem. Cycles*. https://doi.org/10.1029/2019GB006251 (2020).
47. Xu, X. et al. Global greenhouse gas emissions from animal-based foods are twice those of plant-based foods. *Nat. Food* **2**, 724–732 (2021).
48. Gahlot, S. et al. Impact of environmental changes and land management practices on wheat production in India. *Earth Syst. Dyn.* https://doi.org/10.5194/esd-11-641-2020 (2020).
49. Barman, R., Jain, A. K. & Liang, M. Climate-driven uncertainties in modeling terrestrial gross primary production: A site level to global-scale analysis. *Glob Chang. Biol.* https://doi.org/10.1111/gcb.12474 (2014).
50. Gahlot, S., Shu, S., Jain, A. K. & Baidya Roy, S. Estimating Trends and Variation of Net Biome Productivity in India for 1980–2012 Using a Land Surface Model. *Geophys. Res. Lett.* https://doi.org/10.1002/2017GL075777 (2017).
51. Jain, A. K., Meiyappan, P., Song, Y. & House, J. I. CO_2 emissions from land-use change affected more by nitrogen cycle, than by the choice of land-cover data. *Glob Chang. Biol* https://doi.org/10.1111/gcb.12207 (2013).
52. Jagermeyr, J. et al. A regional nuclear conflict would compromise global food security. *Proc. Natl. Acad. Sci. U.S.A.* **117**, 7071–7081 (2020).
53. Masutomi, Y. et al. A land surface model combined with a crop growth model for paddy rice (MATCRO-Rice v. 1) - Part 2: Model validation. *Geosci. Model Dev.* **9**, 4155–4167 (2016).
54. Harris, I., Jones, P. D., Osborn, T. J. & Lister, D. H. Updated high-resolution grids of monthly climatic observations - the CRU TS3.10 Dataset. *Int. J. Climatol.* https://doi.org/10.1002/joc.3711 (2014).
55. Kobayashi, S. et al. The JRA-55 reanalysis: General specifications and basic characteristics. *J. Meteorol. Soc. Japan. Ser. II* **93**, 5–48 (2015).
56. Lobell, D. B. et al. Satellite estimates of productivity and light use efficiency in United States agriculture, 1982-98. *Glob. Chang. Biol.* https://doi.org/10.1046/j.1365-2486.2002.00503.x (2002).
57. Wirsenius, S. *Human use of land and organic materials: modeling the turnover of biomass in the global food system* (Doktorsavhandlingar vid Chalmers Tekniska Hogskola, 2000).
58. Friedlingstein, P. et al. Global Carbon Budget 2021. *Earth Syst. Sci. Data*. **14**, 1917–2005 (2022).
59. Lamarque, J. F. et al. The atmospheric chemistry and climate model intercomparison project (ACCMIP): Overview and description of models, simulations and climate diagnostics. *Geosci. Model Dev.* https://doi.org/10.5194/gmd-6-179-2013 (2013).

Acknowledgements

We thank FLUXNET for providing the following data: (2009-2014) FLUXNET2015 US-Twt Twitchell Island, Dataset (https://doi.org/10.18140/FLX/1440106), and Maricar Alberto, Reiner Wassmann (2012-2014) FLUX NET-CH4 PH-RiF Philippines Rice Institute flooded Dataset (https://doi.org/10.18140/FLX/1669653). We also acknowledge AsiaFlux for providing access to the following data: IRRI Flux Research Site and Mase Paddy Flux site data sets. The authors also thank Dr. Haroon S. Kheshgi for the initial support and discussion of the work.

Author contributions

T.-S.L. and AKJ designed the framework of this study. T.-S.L. collected data, performed the model simulations, and analyzed the results. T.-S.L. and AKJ wrote the paper.

Funding
Funding for this work was provided by the US National Science Foundation's Innovations at the Nexus of Food, Energy, and Water Systems Program (INFEWS/T1 Grant #1856012), and by the NASA Land-Cover and Land-Use Change (LCLUC) Program (NASA Grant Nos. 80NSSC24K0920 and 80NSSC25K7497).

Declarations

Competing interests
The authors declare no competing interests.

Additional information
Supplementary Information The online version contains supplementary material available at https://doi.org/10.1038/s41598-026-55973-0.

Correspondence and requests for materials should be addressed to A.K.J.

Reprints and permissions information is available at www.nature.com/reprints.

Publisher's note Springer Nature remains neutral with regard to jurisdictional claims in published maps and institutional affiliations.

Open Access This article is licensed under a Creative Commons Attribution-NonCommercial-NoDerivatives 4.0 International License, which permits any non-commercial use, sharing, distribution and reproduction in any medium or format, as long as you give appropriate credit to the original author(s) and the source, provide a link to the Creative Commons licence, and indicate if you modified the licensed material. You do not have permission under this licence to share adapted material derived from this article or parts of it. The images or other third party material in this article are included in the article's Creative Commons licence, unless indicated otherwise in a credit line to the material. If material is not included in the article's Creative Commons licence and your intended use is not permitted by statutory regulation or exceeds the permitted use, you will need to obtain permission directly from the copyright holder. To view a copy of this licence, visit http://creativecommons.org/licenses/by-nc-nd/4.0/.

© The Author(s) 2026